Article

The Effects of pH Values on Functional Mechanisms of Nitrite Anions for Q235 Carbon Steels in 0.01 mol L^{-1} NaNO$_2$-HCl Solutions

Yong Zhou, ⓘ *,a Pei Zhang,b Huiju Huang,a Jinping Xiongc and Fuan Yana*

*aKey Laboratory for Green Chemical Process of Ministry of Education,
Wuhan Institute of Technology, 430205 Wuhan, China*

bCollege of Chemistry and Food Science, Yulin Normal University, 537000 Yulin, China

*cBeijing Key Laboratory of Electrochemical Process and Technology for Materials,
Beijing University of Chemical Technology, 100029 Beijing, China*

For Q235 carbon steels in 0.01 mol L^{-1} NaNO$_2$-HCl solutions with different pH values, the effects of pH values on the functional mechanisms of nitrite anions (NO$_2^-$) were studied. In the pH 1 and pH 2 solutions, the Q235 steels showed the electrochemical behavior of activation, and uniform corrosion (UC) was the main corrosion type on the Q235 surface. The presence of NO$_2^-$ did not affect the electrochemical behavior and the corrosion type but only accelerated the anodic reaction of Fe oxidation. In the pH 3 and pH 4 solutions, the Q235 steels presented the electrochemical behavior of activation-passivation transition, and intergranular corrosion (IGC) occurred on the Q235 surface. The cathodic reaction of NO$_2^-$ reduction resulted in the transition of electrochemical behavior from activation to passivation and the change of corrosion type from UC to IGC. In the pH 5 and pH 6 solutions, the Q235 steels exhibited the electrochemical behavior of self passivation-pitting, and pitting corrosion (PC) was present on the Q235 surface. The strong oxidability of NO$_2^-$ played a critical role in the formation of γ-Fe$_2$O$_3$ passive film on the Q235 surface under the combined action of Fe^{2+} and NO$_2^-$.

Keywords: Q235 carbon steel, pH value, NO$_2^-$, corrosion, passivation, polarization

Introduction

Carbon steels are used in the different fields of production and living widely,[1-3] but it is unavoidable that the application and development of carbon steels are limited by the disadvantage of corrosion and failure.[4-6] For carbon steels, the addition of inhibitors into service environments is one of main methods to decrease the corrosion rate,[7] and nitrite anions (NO$_2^-$) are kind of effective inhibitors to restrain the corrosion process.[8]

At present, the studies on the inhibitive effect and mechanism of NO$_2^-$ for carbon steels are mainly focused on alkaline and neutral media, particularly on the corrosion environments of reinforced concrete[9-11] and chloride.[12-14] It is generally accepted that in alkaline and neutral media, the presence of NO$_2^-$ promotes the surface passivation of carbon steels, which is attributed to the mechanism of NO$_2^-$ for repairing the defects in the air-formed oxide film and making the oxide film to grow and re-arrange towards a regular passive film.[8,11,13] However, in acidic media, the related studies involving NO$_2^-$ are relatively few, and the present studies are summarized as follows. In carbon dioxide (CO$_2$) corrosion environments, Zhou *et al.*[15-18] studied the influence of NO$_2^-$ on the corrosion / passivation behavior of Q235 carbon steel in CO$_2$ saturated solution (pH 3.7) in detail. The Q235 steel presented the electrochemical behavior of activation in CO$_2$ saturated solution without NO$_2^-$;[15] after the addition of NO$_2^-$, the electrochemical behavior transferred from activation to anodic passivation, and the critical NO$_2^-$ concentration for the stable passivation was approximately 0.05 mol L^{-1};[16] intergranular corrosion (IGC) was observed on the surface of Q235 carbon steel when the Q235 steel was polarized into activation-passivation potential region with a low potential scanning rate;[17] the occurrence of IGC was very closely associated with the electrochemical behavior of activation-passivation transition, which was resulted from the synergetic mechanisms of CO$_2$ and NO$_2^-$.[18] In other

*e-mail: zhouyong@wit.edu.cn

acidic media, Zuo *et al.*[19] studied the combined influences of NO_2^- and thioureido imidazoline (TAI) on the passivation behavior and the pitting corrosion (PC) of X70 carbon steels in acidic NaCl solution (pH 5.5) and reported that the mechanisms of NO_2^- and TAI were both interactive and superimposed, and the addition of NO_2^- was beneficial to restrain the initiation and propagation of PC. Nevertheless, the detailed mechanism of NO_2^- was not discussed further. Garces *et al.*[20] studied the influence of NO_2^- on the propagation of PC for the corrugated steel bar in simulated pit solution (pH 1.46-6.38). The authors reported that the addition of NO_2^- showed a limited inhibition for the pit propagation, but the excessive addition even increased the uniform corrosion (UN) rate. However, due to the complicated component of simulated pit solution, the mechanism of NO_2^- was not completely clear.

From the above statements, although the studies about the mechanism of NO_2^- for the corrosion and passivation of carbon steels in acidic media are present, the pH values of acidic media are relatively single and not systematic. Therefore, it is necessary to carry out the detailed discussion for the mechanism of NO_2^- in the entire acidic pH range. At the same time, in our previous study,[8] it was reported that the critical NO_2^- concentration of stable passivation for the Q235 steel in pure nitrite solution was 0.01 mol L^{-1}. Based on this result, in this work, diluted hydrochloric acid is introduced into 0.01 mol L^{-1} $NaNO_2$ solution to adjust pH value, and 0.01 mol L^{-1} $NaNO_2$-HCl solutions with different pH values are obtained. Further, the effects of pH values on the functional mechanisms of NO_2^- for Q235 carbon steels in the above solutions are studied by electrochemical measurements and microstructure observations, and the related mechanisms of electrochemical behavior and localized corrosion are also discussed.

Experimental

The tested material was Q235 carbon steel with the following chemical composition (wt.%): C, 0.160; Mn, 0.530; Si, 0.300; S, 0.045; P, 0.015, and Fe, 98.950. Samples were manually abraded up to 1000 grit with SiC abrasive papers, rinsed with de-ionized water and degreased in alcohol.

The tested electrolyte was 0.01 mol L^{-1} $NaNO_2$-HCl solutions with different pH values which were adjusted to acidic range from pH 1 to 6 with the introduction of diluted hydrochloric acid into 0.01 mol L^{-1} $NaNO_2$ solution.

The electrochemical measurements of polarization curve, electrochemical impedance spectroscopy (EIS) and Mott-Schottky plot were carried out using a CS350 electrochemical workstation (China). A typical three electrode system was applied for all the electrochemical measurements. The system was composed of a saturated calomel electrode (SCE) as reference electrode, a platinum sheet as counter electrode and a Q235 sample as working electrode. Before each electrochemical test, the working electrode was immersed in the corresponding tested electrolyte for a certain period of time until the open circuit potential (OCP) was stable. In the polarization curve test, the potential scanning rate was 0.1 mV s^{-1}, and the potential scanning range was from -0.3 V_{OCP} to the potential value corresponding to the objective electrochemical characteristic. In the EIS test, a perturbation potential of 10 mV amplitude was applied in the frequency range from 10^5 to 10^{-2} Hz. In the Mott-Schottky plot test, the potential scanning rate was 5.0 mV s^{-1}, and the potential scanning range was from -0.2 to 1.2 V_{SCE}. All of the electrochemical measurements were carried out at 25 ºC, which was controlled with an electro-thermostatic water bath.

The surface morphologies were observed by a SU1510 scanning electron microscope (SEM) instrument (Japan), and the surface composition was detected by a Kevex SuperDry energy dispersion X-ray spectroscopy (EDS) instrument attached on the SEM system.

Results and Discussion

Electrochemical behavior and corrosion type

Figure 1 shows the polarization curves and the EIS of Q235 samples in 0.01 mol L^{-1} $NaNO_2$-HCl solutions with different pH values. From Figure 1a, the effects of pH values on the electrochemical behaviors are very significant: the Q235 samples presented the electrochemical behaviors of activation, activation-passivation transition and self passivation-pitting in the solutions with pH 1 and 2, pH 3 and 4, and pH 5 and 6, respectively. It may suggest the different mechanisms of NO_2^- for Q235 carbon steels in acidic pH range. At the same time, under the different electrochemical behaviors, the effects of pH values on the electrochemical parameters, including corrosion potential (E_{corr}), corrosion current density (i_{corr}), activation-passivation transition potential (E_{trans}), passive current density (i_{pass}) and pitting potential (E_{pit}), are also prominent.

Table 1 lists the effects of pH values on the electrochemical behavior and the electrochemical parameter value. From Table 1, with the increase of pH value, the E_{corr} value moves to the positive direction and the i_{corr} value decreases obviously, indicating the decreased rate of UC with the increased pH value.[21] Similar results are also confirmed by the EIS data, which will be discussed later. Besides, in the solutions from pH 3 to 6, under
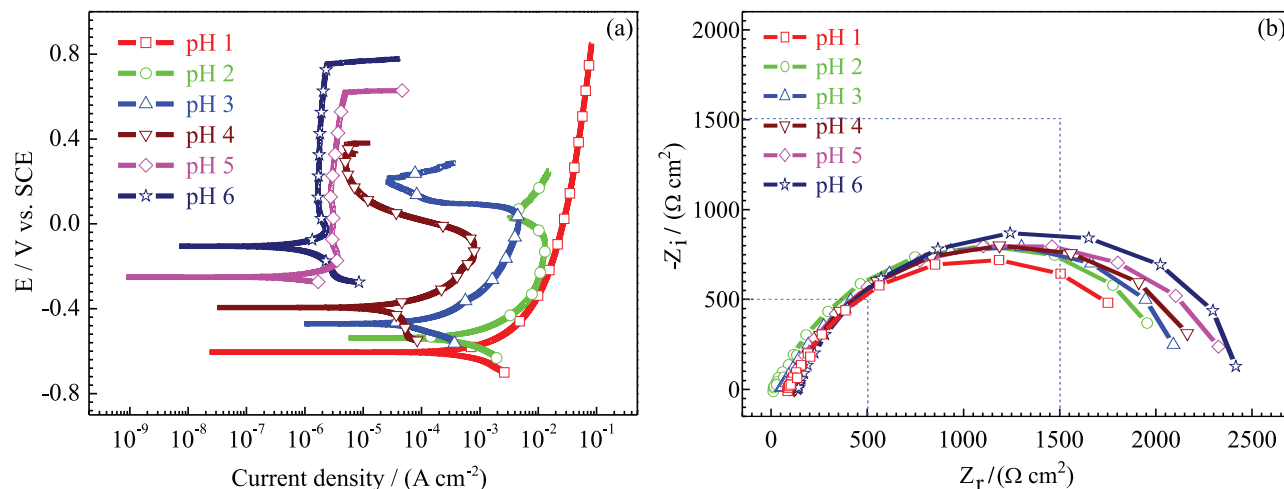
Figure 1. Polarization curves and EIS of Q235 samples in 0.01 mol L^{-1} NaNO$_2$-HCl solutions with different pH values: (a) polarization curves and (b) EIS.

the electrochemical behaviors of activation-passivation transition and self passivation-pitting, the negative direction of E$_{trans}$ and the decrease of i$_{pass}$ are present with the increase of pH value, suggesting that the passivation occurred in the solution with high pH value is easier than that in the solution with low pH value.

From Figure 1b, all of Nyquist plots for the EIS are composed of only depressed capacitive loop at the tested frequency range, which was independent on the pH values. It was reported that the characteristic of capacitive loop reflected the corrosion resistance of surface protection film on metals and alloys.[16] Figure 1b illustrates that the radius of capacitive loop enlarges with the increase of pH value, indicating that the corrosion resistance of surface protection film formed in the high pH solution is greater than that formed in the low pH solution, which is in agreement with the results of E$_{corr}$ and i$_{corr}$. Further, in order to confirm the above discussion, the equivalent electrical circuit (EEC) fitting is also performed. According to the Nyquist plots shown in Figure 1b and the previous study,[8] the EEC model shown in Figure 2 is applied to fit the EIS, in which R$_S$ represents the solution resistance, and R$_f$ and CPE$_f$ represent the resistance and the capacitance of surface protection film, respectively.
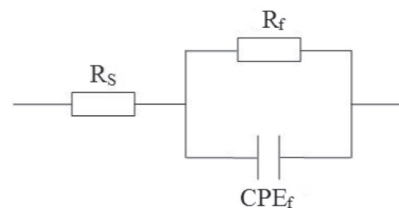

Figure 2. Equivalent electrical circuit model.

Table 2 lists the calculated values of R$_f$ from the EEC fitting. From Table 2, the R$_f$ value increases with the increased pH value, confirming the faster rate of UC in the low pH solution than in the high pH solution.

Figure 3 shows the surface SEM morphologies of Q235 samples in 0.01 mol L^{-1} NaNO$_2$-HCl solutions with different pH values when the values of anodic current density in the polarization curve tests reach 0.1 A cm^{-2}. From Figures 3a and 3b, except some parallel scratches attributed to the mechanical action of abrasive paper, no localized corrosion feature is observed on the sample surface, which is consistent with the results shown in Figure 1a that the Q235 steels showed the electrochemical behavior of activation in the pH 1 and 2 solutions. Further, the scratches shown in Figure 3b is more obvious and abundant than those shown in Figure 3a, which is due to the dissolution rate of Q235

Table 1. Effects of pH values on electrochemical behavior and electrochemical parameter value

pH value	Electrochemical behavior	E$_{corr}$ / V$_{SCE}$	i$_{corr}$ / (A cm^{-2})	E$_{trans}$ / V$_{SCE}$	i$_{pass}$ / (A cm^{-2})	E$_{pit}$ / V$_{SCE}$
1	activation	−0.61	4.55×10^{-3}	–	–	–
2	activation	−0.53	1.69×10^{-3}	–	–	–
3	activation-passivation	−0.47	3.23×10^{-4}	0.04	2.91×10^{-5}	–
4	activation-passivation	−0.39	7.81×10^{-5}	−0.11	4.92×10^{-6}	–
5	self passivation-pitting	−0.25	3.25×10^{-6}	–	3.25×10^{-6}	0.62
6	self passivation-pitting	−0.11	1.75×10^{-6}	–	1.75×10^{-6}	0.76

E$_{corr}$: corrosion potential; i$_{corr}$: corrosion current density; E$_{trans}$: activation-passivation transition potential; i$_{pass}$: passive current density; E$_{pit}$: pitting potential.

Table 2. Calculated values of surface protection film resistance from EEC fitting

pH value	R_f / (Ω cm^2)
1	1750.85
2	1954.58
3	2091.90
4	2162.67
5	2326.45
6	2415.71

R_f: resistance of surface protection film.

carbon steel is quicker in the pH 1 solution than in the pH 2 solution, confirmed by the values of anodic current density shown on the polarization curves in Figure 1a.

From Figures 3c and 3d, obvious corrosion dissolution along grain boundaries is observed on the sample surface, indicating the occurrence of IGC for the Q235 steels in the pH 3 and 4 solutions. Similar results were also reported in our previous study: for Q235 carbon steel in $NaNO_2$-CO_2 solution with 0.01 mol L^{-1} NO_2^- and pH 3.7, the occurrence of IGC was observed on the Q235 surface when the Q235 steel was polarized into activation-passivation potential
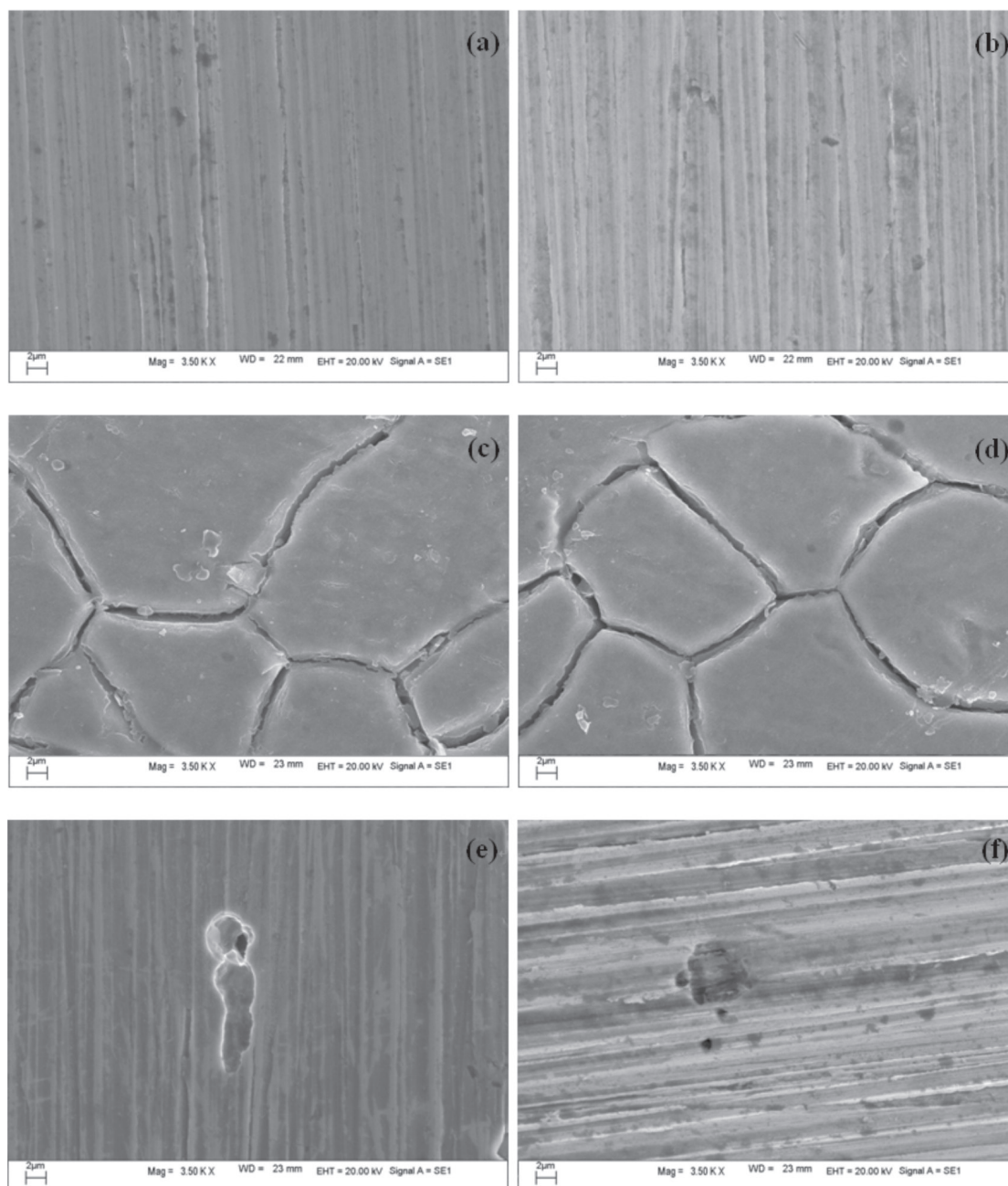

Figure 3. Surface SEM morphologies of Q235 samples in 0.01 mol L^{-1} $NaNO_2$-HCl solutions with different pH values when values of anodic current density in polarization curve tests reach 0.1 A cm^{-2}: pH (a) 1, (b) 2, (c) 3, (d) 4, (e) 5 and (f) 6.

region.[17] From Figure 1a, the electrochemical behavior of activation-passivation transition is also present when the Q235 steels were polarized in the pH 3 and 4 solutions. Therefore, by referring to the previous study,[17] the mechanisms of NO_2^- for the electrochemical behavior of activation-passivation transition and the occurrence of IGC can be clarified, which will be discussed later.

From Figures 3e and 3f, for the Q235 steels in the pH 5 and 6 solutions, the presence of corrosion pits is observed on the sample surface obviously, indicating the occurrence of PC. It is in agreement with the results shown in Figure 1a that the electrochemical behavior of self passivation-pitting is present on the polarization curves in the pH 5 and 6 solutions. Further, EDS analysis revealed that the elements of Mn, S and Cl were present within each pit. It is generally accepted that for carbon steels in chloride solutions, the initiation and propagation of PC is very closely related to the adsorption of Cl^- at MnS inclusions.[22-24] Besides Cl^-, NO_2^- is responsible for the formation of passive film on the surface of carbon steels,[25] which also plays a critical role in the occurrence of PC.

From the results shown in Figures 1 and 3, for Q235 carbon steels in 0.01 mol L^{-1} NaNO$_2$-HCl solutions, the effects of pH values on the electrochemical behavior and the corrosion type are very prominent, which are list in Table 3. The above results also suggest the different mechanisms of NO_2^- for carbon steels in the entire acidic pH range. The effects of pH values on the functional mechanisms of NO_2^- for the Q235 steels will be discussed as follows.

Table 3. Effects of pH values on electrochemical behavior and corrosion type for Q235 carbon steels in 0.01 mol L^{-1} NaNO$_2$-HCl solutions

pH value	Electrochemical behavior	Corrosion type
1 and 2	activation	uniform corrosion (UC)
3 and 4	activation-passivation transition	intergranular corrosion (IGC)
5 and 6	self passivation-pitting	pitting corrosion (PC)

NO_2^- mechanism in 0.01 mol L^{-1} NaNO$_2$-HCl solutions with pH 1 and 2

In order to understand the mechanisms of NO_2^- in 0.01 mol L^{-1} NaNO$_2$-HCl solutions with pH 1 and 2, two Q235 samples were polarized in the pH 1 NaNO$_2$-HCl solution and the pH 1 pure HCl solution, respectively.

Figure 4 shows the polarization curves of Q235 samples in the pH 1 NaNO$_2$-HCl solution and the pH 1 pure HCl solution. Both samples showed the same electrochemical behavior of activation in the corresponding tested solutions.

However, it is noteworthy that at the same applied potential, the value of anodic current density for the Q235 sample in the pH 1 NaNO$_2$-HCl solution is greater than that in the pH 1 pure HCl solution, suggesting the mechanism of NO_2^- to accelerate the electrode process.

For carbon steels in acidic media, the main anodic and cathodic reactions are as follows:

$$Fe \rightarrow Fe^{2+} + 2e \qquad (1)$$
$$2H^+ + 2e \rightarrow H_2 \qquad (2)$$

It was reported that the cathodic process was accelerated when NO_2^- was present in acidic media, which was due to the following cathodic reaction:[26]

$$NO_2^- + 2H^+ + e \rightarrow NO + H_2O \qquad (3)$$

Because the equilibrium potential of NO_2^- reduction (equation 3) is more positive than that of H^+ reduction (equation 2),[26] the cathodic process is accelerated derived from the addition of NO_2^-, further resulting in that the anodic reaction of Fe oxidation (equation 1) moves to the right direction. Therefore, the higher value of anodic current density for the Q235 steel is observed in the pH 1 NaNO$_2$-HCl solution than in the pH 1 pure HCl solution, as shown in Figure 4.
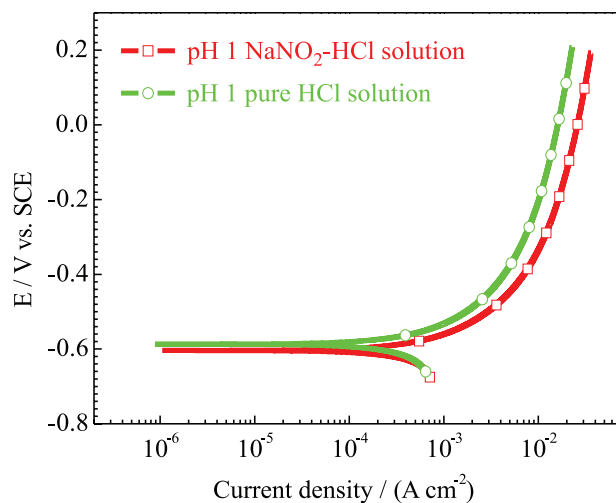

Figure 4. Polarization curves of Q235 samples in pH 1 NaNO$_2$-HCl solution and in pH 1 pure HCl solution.

In 0.01 mol L^{-1} NaNO$_2$-HCl solutions with pH 1 and 2, besides H^+ and NO_2^-, the presence of Cl^- is not neglected, which may greatly affect the electrochemical behaviors of Q235 carbon steels.[27] In order to clarify the effect of Cl^-, the application of diluted nitric acid was performed to adjust the pH values of 0.01 mol L^{-1} NaNO$_2$-HNO$_3$ solutions.

Figure 5 shows the polarization curves of Q235 samples in 0.01 mol L^{-1} NaNO$_2$-HCl solutions and in 0.01 mol L^{-1} NaNO$_2$-HNO$_3$ solutions with pH 1 and 2. From Figure 5, the Q235 samples showed the electrochemical behavior of activation-passivation-transpassivation when the solution acidity was adjusted with diluted nitric acid. The change of electrochemical behavior from the activation in the pH 1 and 2 NaNO$_2$-HCl solutions to the activation-passivation-transpassivation in the pH 1 and 2 NaNO$_2$-HNO$_3$ solutions confirms that the presence of Cl$^-$ also plays a critical role in the electrochemical behavior and the corrosion type for the Q235 steels in 0.01 mol L^{-1} NaNO$_2$-HCl solutions with pH 1 and 2.

Further, from Figure 5, besides on the polarization curves in the pH 1 and 2 NaNO$_2$-HNO$_3$ solutions, the electrochemical behavior of activation-passivation transition occurring at the potential value of 0 V$_{SCE}$ is also observed on the polarization curve in the pH 2 NaNO$_2$-HCl solution. However, it is worth noting that the activation-passivation transition region is not complete, and the anodic current density increases suddenly once again after the applied potential exceeds 0 V$_{SCE}$. Therefore, it can be inferred that in the pH 1 and 2 NaNO$_2$-HCl solutions, in the potential range from E$_{corr}$ to 0 V$_{SCE}$, the presence of H$^+$ may dominate the anodic process of Q235 carbon steel; after the potential value of 0 V$_{SCE}$, the presence of Cl$^-$ does it. Nevertheless, the detailed combined effects of H$^+$ and Cl$^-$ need to be studied further.
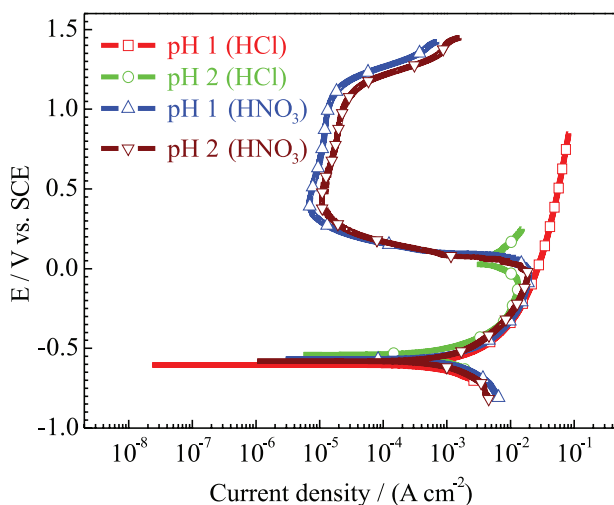

Figure 5. Polarization curves of Q235 samples in 0.01 mol L^{-1} NaNO$_2$-HCl solutions and in 0.01 mol L^{-1} NaNO$_2$-HNO$_3$ solutions with pH 1 and 2.

From the above results, for Q235 carbon steels in 0.01 mol L^{-1} NaNO$_2$-HCl solutions with pH 1 and 2, the presence of NO$_2^-$ do not affect the electrochemical behavior and the corrosion type but only accelerate the anodic reaction of Fe oxidation.

NO$_2^-$ mechanism in 0.01 mol L^{-1} NaNO$_2$-HCl solutions with pH 3 and pH 4

As shown in Figure 4, the Q235 steel showed the electrochemical behavior of activation in the pH 1 pure HCl solution, and the same electrochemical behaviors are also observed in pure HCl solutions from pH 2 to 6. In contrast, from Figure 1a, the Q235 steels presented the electrochemical behavior of activation-passivation transition in the pH 3 and 4 NaNO$_2$-HCl solutions. The significant change of electrochemical behavior is attributed to the presence of NO$_2^-$.

For Q235 carbon steels in 0.01 mol L^{-1} NaNO$_2$-HCl solutions with pH 3 and 4, the electrochemical behavior of activation-passivation transition and the occurrence of IGC are present, which is similar to our previous study on the corrosion behavior of Q235 carbon steel in 0.01 mol L^{-1} NaNO$_2$-CO$_2$ solution with pH 3.7.[17] In order to confirm the similar mechanism of NO$_2^-$, or not, in the pH 3.7 NaNO$_2$-CO$_2$ solution and in the pH 3 and 4 NaNO$_2$-HCl solutions, the polarization curve test for the Q235 steel in the pH 3.7 NaNO$_2$-HCl solution is carried out, as shown in Figure 6.
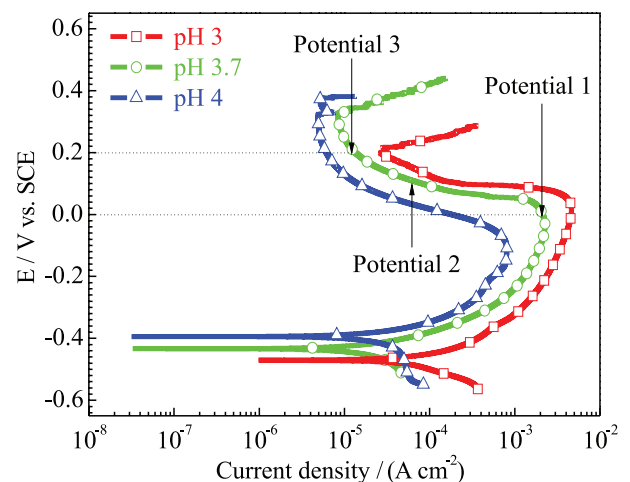

Figure 6. Polarization curves of Q235 samples in 0.01 mol L^{-1} NaNO$_2$-HCl solutions with pH 3, 3.7 and 4.

From Figure 6, besides the sudden increase of anodic current density in the stable passivation region due to the presence of Cl$^-$,[28] the polarization curve for the Q235 steel in the pH 3.7 NaNO$_2$-HCl solution exhibits the highly similar rule to that in the pH 3.7 NaNO$_2$-CO$_2$ solution.[17] Further, the same electrochemical behavior is also observed on the polarization curves of Q235 carbon steels in the pH 3, 3.7 and 4 NaNO$_2$-HCl solutions. The above results indicate the similar mechanism of NO$_2^-$ for Q235 carbon steels in NaNO$_2$-CO$_2$ solution and in NaNO$_2$-HCl solutions, which is discussed as follows.

Besides the cathodic reaction of NO_2^- reduction (equation 3), it was reported that the following cathodic reaction was present in acidic media:[29]

$$NO_2^- + e \rightarrow NO + O^{2-} \qquad (4)$$

Further, it was reported that in the pH 3.7 $NaNO_2$-CO_2 solution, the equilibrium potential of equation 4 (0.715 V_{SCE}) was more positive than that of equation 3 (0.429 V_{SCE}) and that of equation 1 (−0.684 V_{SCE}), resulting in the following reaction spontaneously:[17]

$$Fe^{2+} + NO_2^- \rightarrow Fe^{3+} + NO + O^{2-} \qquad (5)$$
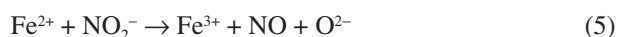
Therefore, for the Q235 steels in the pH 3, 3.7 and 4 $NaNO_2$-HCl solutions, the presence of equation 5 is responsible for the electrochemical behavior of activation-passivation transition, as shown in Figure 6. At the same time, due to the enrichment of Fe in grain interiors and the segregation of Si and Mn in grain boundaries, the occurrence of IGC is observed on the Q235 surface when the electrochemical behavior of activation-passivation transition is present,[17] as shown in Figures 3c and 3d. In order to further confirm the same mechanism of NO_2^- in the pH 3.7 $NaNO_2$-CO_2 solution and in the pH 3 and 4 $NaNO_2$-HCl solutions, the application of SEM is performed to observe the Q235 samples polarized to different potentials in the pH 3.7 $NaNO_2$-HCl solution, and the detailed potentials are marked on the polarization curve, as shown in Figure 6.

From Figure 7a, when the Q235 sample was polarized to potential 1 (0 V_{SCE}), the occurrence of IGC is observed on the Q235 surface but with a moderate degree: only parts of grain boundaries are damaged and the attacked grain boundaries are discontinuous. Further, from Figures 7b and 7c, all of grain boundaries are damaged and the dissolved grain boundaries form a complete network when the Q235 samples were polarized to potential 2 (0.1 V_{SCE})

and potential 3 (0.2 V_{SCE}), and the IGC degree for the Q235 sample polarized to potential 3 is more serious than that polarized to potential 2. The IGC process of Q235 carbon steel in the pH 3.7 $NaNO_2$-HCl solution is consistent with that in the pH 3.7 $NaNO_2$-CO_2 solution, confirming the same mechanism of NO_2^-.

However, it needs to clarify that in our previous study, it was reported that the occurrence of IGC was attributed to the combined effects of CO_2 and NO_2^-, and NO_2^- promoted the passivation on the surface of crystal grains but CO_2 induced the dissolution at the vicinity of grain boundaries.[17] In this work, according to the results shown in Figures 6 and 7, it is H^+, rather than CO_2, to cause the dissolution of grain boundaries.

From the above results, for Q235 carbon steels in 0.01 mol L^{-1} $NaNO_2$-HCl solutions with pH 3 and 4, the cathodic reaction of NO_2^- reduction results in the transition of electrochemical behavior from activation to passivation and the change of corrosion type from UC to IGC.

NO_2^- mechanism in 0.01 mol L^{-1} $NaNO_2$-HCl solutions with pH 5 and pH 6

For Q235 carbon steels in 0.01 mol L^{-1} $NaNO_2$-HCl solutions with pH 5 and 6, the electrochemical behavior of self passivation-pitting and the occurrence of PC are present, as shown in Figures 1a, 3e and 3f. By contrast, the Q235 steels presented the electrochemical behavior of activation in pure HCl solutions with pH 5 and 6. The above results suggest the mechanism of NO_2^- during the process of PC.

It was reported that for the occurrence of PC on the surface of carbon steels, the formation of passive film on the steel surface and the presence of aggressive anions in the service environment were two essential factors.[12] In this work, for the Q235 steels in the pH 5 and 6 $NaNO_2$-HCl solutions, the above two factors are present.
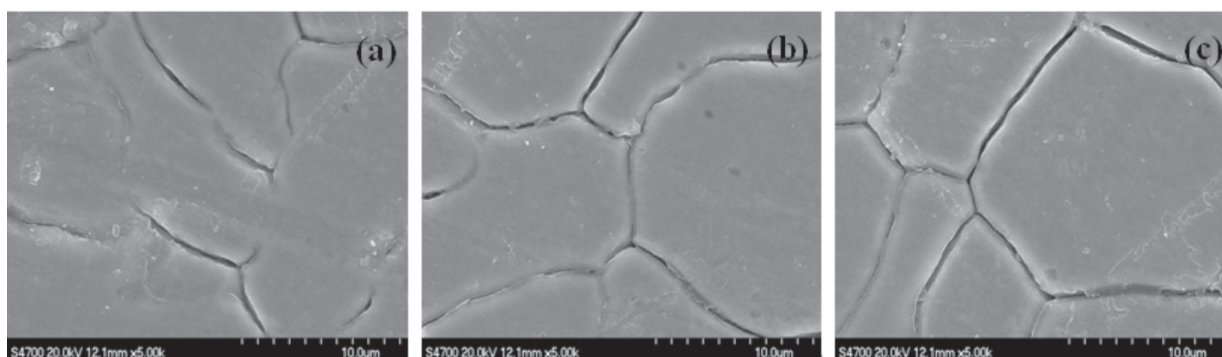

Figure 7. Surface SEM morphologies of Q235 samples polarized to different potentials in 0.01 mol L^{-1} $NaNO_2$-HCl solution with pH 3.7: (a) potential 1 (0 V_{SCE}), (b) potential 2 (0.1 V_{SCE}) and (c) potential 3 (0.2 V_{SCE}).

In alkaline and neutral media containing NO_2^-, carbon steels usually shows the electrochemical behavior of self passivation[8] and the γ-Fe_2O_3 passive film is formed on the steel surface,[9] which is attributed to the following reaction:[14]

$$2Fe^{2+} + 2OH^- + 2NO_2^- \rightarrow 2NO + \gamma\text{-}Fe_2O_3 + H_2O \qquad (6)$$

From Figure 1a, the electrochemical behavior of self passivation is also observed on the polarization curves for the Q235 steels in pH 5 and pH 6 solutions before the applied potential is up to E_{pit}, indicating the occurrence of equation 6 on the Q235 surface. At the same time, the other factor of PC, aggressive Cl^-, is also present, which is introduced during the process of adjusting pH value with diluted hydrochloric acid. Therefore, the combined actions of passive film and aggressive Cl^- result in the electrochemical behavior of self passivation-pitting and the occurrence of PC, the mechanism of NO_2^- is attributed to its contribution for the formation of γ-Fe_2O_3 passive film on the Q235 surface.

However, as shown in Figure 1a and Table 1, the value of E_{pit} for the Q235 steel in the pH 5 solution is more negative than that in the pH 6 solution, which is due to the different concentrations of OH^- and Cl^- in the pH 5 and 6 solutions. Because of different amount of diluted hydrochloric acid to adjust pH value, the concentrations of OH^- and Cl^- in the pH 5 solution are lower and higher than those in the pH 6 solution, respectively.

On the one hand, the higher OH^- concentration in the pH 6 solution than in the pH 5 solution results in the different extent of equation 6 in the two solutions. It is inferred that the corrosion resistance of passive film formed in the pH 6 solution is better than that formed in the pH 5 solution, which can be confirmed by the film resistance and the film defect. From Table 2, the R_f value for the Q235 steel in the pH 6 solution is higher than that in the pH 5 solution, indicating that the corrosion resistance of passive film formed in the pH 6 solution is greater than that formed in the pH 5 solution.[30] Besides film resistance, the electrochemical test of Mott-Schottky plot is also performed to characterize the film defect.

Figure 8 shows the Mott-Schottky plots of Q235 samples in 0.01 mol L^{-1} $NaNO_2$-HCl solutions with pH 5 and 6. From Figure 8, the slopes of straight line parts on the both Mott-Schottky plots show positive values, indicating that the passive film on the surface of Q235 carbon steels is an n-type semiconductor.[31] For n-type semiconductors, the following equation can be applied to interpret Mott-Schottky plot:

$$\frac{1}{C_{sp}^2} = \frac{2\left(E_{apply} - U_{fb} - \dfrac{kT}{e}\right)}{\varepsilon\varepsilon_0 e N_D} \qquad (7)$$

In equation 7, C_{sp} represents the space electron layer capacitance, E_{apply} represents the applied potential, U_{fb} represents the flat band potential, k is the Boltzmann constant, T is the absolute temperature, e is the electron charge, ε is the dielectric constant of passive film, ε_0 is the permittivity of free space, and N_D represents the donor density.

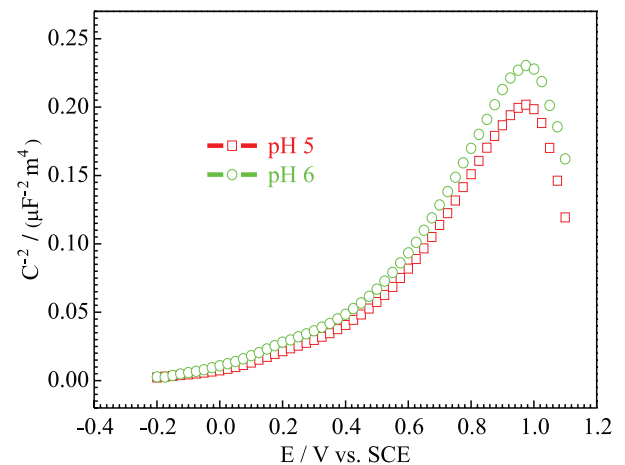**Figure 8.** Mott-Schottky plots of Q235 samples in 0.01 mol L^{-1} $NaNO_2$-HCl solutions with pH 5 and 6.

It was reported that the defect of passive film was closely associated with the value of N_D, which was inversely proportional to the slope of straight line part on the Mott-Schottky plot.[32] From Figure 8, the slope of straight line part for the Q235 steel in the pH 6 solution is greater than that in the pH 5 solution, indicating the defect of passive film formed in the pH 6 solution is less than that formed in the pH 5 solution. The above results of film resistance and film defect confirm that the corrosion resistance of passive film formed in the pH 6 solution is larger than that formed in the pH 5 solution.

On the other hand, the Cl^- concentrations in the pH 5 and 6 solutions before and after the polarization curve tests were measured, as shown in Figure 9. Both before and after the polarization curve tests, the Cl^- concentration in the pH 5 solution is higher than that in the pH 6 solution, which is also responsible for the more negative of E_{pit} for the Q235 steel in the pH 5 solution than in the pH 6 solution.

Conclusions

In this work, the effects of pH values on the mechanisms of NO_2^- for Q235 carbon steels in 0.01 mol L^{-1} $NaNO_2$-HCl

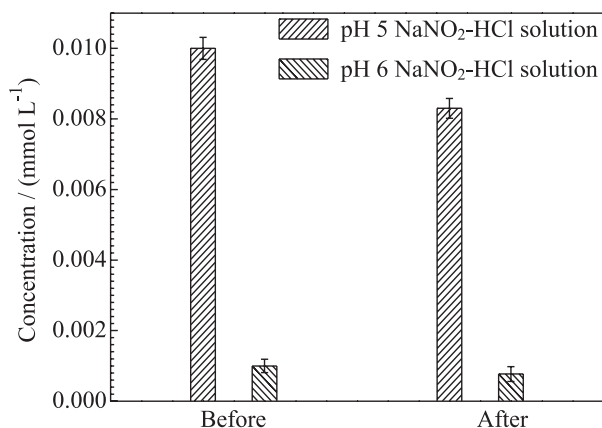**Figure 9.** Concentrations of Cl$^-$ in 0.01 mol L^{-1} NaNO$_2$-HCl solutions with pH 5 and 6 before and after polarization curve tests.

solutions with different pH values were studied, and the related mechanisms of electrochemical behavior and localized corrosion were also discussed. In the pH 1 and 2, pH 3 and 4, and pH 5 and 6 NaNO$_2$-HCl solutions, the Q235 steels showed the electrochemical behaviors of activation, activation-passivation transition and self passivation-pitting, respectively corresponding to the occurrence of UC, IGC and PC. The effects of pH values on the mechanisms of NO$_2^-$ were very significant. The presence of NO$_2^-$ did not affect the electrochemical behavior and the corrosion type but only accelerated the anodic reaction of Fe oxidation in the pH 1 and 2 solutions. In the pH 3 and 4 solutions, the transition of electrochemical behavior from activation to passivation and the change of corrosion type from UC to IGC were attributed to the cathodic reaction of NO$_2^-$ reduction. In the pH 5 and 6 solutions, the strong oxidability of NO$_2^-$ played a critical role in the formation of γ-Fe$_2$O$_3$ passive film under the combined action of Fe^{2+} and NO$_2^-$.

Acknowledgments

References

1. Feng, B.; Kang, Y. H.; Sun, Y. H.; Yang, Y.; Yan, X. Z.; *Int. J. Appl. Electromagn. Mech.* **2016**, *52*, 357.

2. Zheng, X. T.; Wu, K. W.; Wang, W.; Yu, J. Y.; Xu, J. M.; Ma, L. W.; *Nucl. Eng. Des.* **2017**, *314*, 285.

3. Shi, J.; Shi, J. F.; Chen, H. X.; He, Y. B.; Wang, Q. J.; Zhang, Y.; *Trans. ASME: J. Pressure Vessel Technol.* **2018**, *140*, 031404.

4. Huang, H. L.; Tian, J.; *Microelectron. Reliab.* **2017**, *78*, 131.

5. Jiang, S. Y.; Ding, H. Q.; Xu, J.; *Trans. ASME, J. Tribol.* **2017**, *139*, 014501.

6. Huang, H. L.; Pan, Z. Q.; Qiu, Y. B.; Guo, X. P.; *Microelectron. Reliab.* **2013**, *53*, 1149.

7. Zhong, P.; Ping K. F.; Qiu, X. H.; Chen, F. X.; *Desalin. Water Treat.* **2017**, *93*, 109.

8. Zhou, Y.; Huang, H. J.; Zhang, P.; Liu, D.; Yan, F. A.; *Surf. Rev. Lett.* **2019**, *26*, 1850218.

9. Dong, Z. H.; Shi, W.; Zhang, G. A.; Guo, X. P.; *Electrochim. Acta* **2011**, *56*, 5890.

10. Garces, P.; Saura, P.; Zornoza, E.; Andrade, C.; *Corros. Sci.* **2011**, *53*, 3991.

11. Dong, Z. H.; Shi, W.; Guo, X. P.; *Corros. Sci.* **2011**, *53*, 1322.

12. Zhou, Y.; Zuo, Y.; *Appl. Surf. Sci.* **2015**, *353*, 924.

13. Reffass, M.; Sabot, R.; Jeannin, M.; Berziou, C.; Refait, P.; *Electrochim. Acta* **2007**, *52*, 7599.

14. Valcarce, M. B.; Vazquez, M.; *Electrochim. Acta* **2008**, *53*, 5007.

15. Zhou, Y.; Zhang, P.; Zuo, Y.; Liu, D.; Yan, F.; *J. Braz. Chem. Soc.* **2017**, *28*, 2490.

16. Zhou, Y.; Zuo, Y.; *J. Electrochem. Soc.* **2015**, *162*, C47.

17. Zhou, Y.; Zuo, Y.; *Electrochim. Acta* **2015**, *154*, 147.

18. Zhou, Y.; Yan, F. A.; *Int. J. Electrochem. Sci.* **2016**, *11*, 3976.

19. Zuo, Y.; Yang, L.; Tan, Y. J.; Wang, Y. S.; Zhao, J. M.; *Corros. Sci.* **2017**, *120*, 99.

20. Garces, P.; Saura, P.; Mendez, A.; Zornoza, E.; Andrade, C.; *Corros. Sci.* **2008**, *50*, 498.

21. Deng, F. G.; Wang, L. S.; Zhou, Y.; Gong, X. H.; Zhao, X. P.; Hu, T.; Wu, C. G.; *RSC Adv.* **2017**, *7*, 48876.

22. Chen, X.; Xiong, Q. Y.; Feng, Z.; Li, H.; Liu, D.; Xiong, J. P.; Zhou, Y.; *Int. J. Electrochem. Sci.* **2018**, *13*, 1656.

23. Feng, X. G.; Lu, X. Y.; Zuo, Y.; Zhuang, N.; Chen, D.; *Corros. Sci.* **2016**, *103*, 223.

24. Chen, L. C.; Zhang, P.; Xiong, Q. Y.; Zhao, P.; Xiong, J. P.; Zhou, Y.; *Int. J. Electrochem. Sci.* **2019**, *14*, 919.

25. Li, Y.; Ma, H.; Cheng, L.; Yu, D.; *Electron. Lett.* **2018**, *54*, 383.

26. Li, X. J.; Gui, F.; Cong, H. B.; Brossia, C. S.; Frankel, G. S.; *Electrochim. Acta* **2014**, *117*, 299.

27. Chen, F. X.; Xie, S. L.; Huang, X. L.; Qiu, X. H.; *J. Hazard. Mater.* **2017**, *322*, 152.

28. Xiong, Q. Y.; Xiong, J. P.; Zhou, Y.; Yan, F. A; *Int. J. Electrochem. Sci.* **2017**, *12*, 4238.

29. Chalamet, A.; *Ann. Chim.* **1973**, *8*, 353.

30. Zhou, Y.; Xiong, J. P.; Yan, F. A.; *Surf. Coat. Technol.* **2017**, *328*, 335.

31. Zheng, Y.; Ling, D.; Wang, Y. W.; Jang, S. S.; Tao, B.; *IEEE Trans. Semicond. Manuf.* **2017**, *30*, 8.

32. Xiong, Q. Y.; Zhou, Y.; Xiong, J. P.; *Int. J. Electrochem. Sci.* **2015**, *10*, 8454.